

# Truncated thermalization of optical waves through supercontinuum generation in photonic crystal fibers

Benoit Barviau<sup>1</sup>, Josselin Garnier<sup>2</sup>, Gang Xu<sup>3</sup>, Bertrand Kibler<sup>3</sup>, Guy Millot<sup>3</sup>, and Antonio Picozzi<sup>3</sup>

<sup>1</sup>*Complexe de Recherche Interprofessionnel en Aérothermochimie - University of Rouen, Rouen, France*

<sup>2</sup>*Ecole Normale Supérieure, Applied Mathematics Dept., CNRS, 45 rue d'Ulm, Paris, France*

<sup>3</sup>*Laboratoire Interdisciplinaire Carnot de Bourgogne, CNRS-Université de Bourgogne, Dijon, France*

We revisit the process of optical wave thermalization through supercontinuum generation in photonic crystal fibers. We report theoretically and numerically a phenomenon of ‘truncated thermalization’: The optical wave exhibits an irreversible evolution toward a Rayleigh-Jeans thermodynamic equilibrium state characterized by a compactly supported spectral shape. This phenomenon sheds new light on the mechanism underlying the formation of bounded SC spectra in photonic crystal fibers.

PACS numbers: 42.65.Ky, 42.65.Sf, 42.81.Dp

*Introduction.*— The propagation of partially coherent nonlinear optical waves is a subject of growing interest in different fields of investigations, such as, e.g., wave propagation in homogeneous [1–3] or periodic media [4], nonlinear imaging [5], cavity systems [6–8], or nonlinear interferometry [9]. Owing to their highly nonlinear properties, photonic crystal fibers (PCF) offer unique perspectives for the experimental study of incoherent optical waves over large nonlinear propagation lengths. Indeed, light propagation in PCFs nearby a zero-dispersion wavelength (ZDW) is characterized by a dramatic spectral broadening, a phenomenon termed supercontinuum (SC) generation [10]. Although the interpretation of the mechanisms underlying SC generation in PCFs are rather well understood, a satisfactory theoretical description of SC generation is still lacking, due to the multitude of nonlinear effects underlying this process. However, there is a growing interest in developing new theoretical approaches aimed at describing SC generation in more details, such as, e.g., soliton induced dispersive wave generation [11–14], the effective three-wave mixing theory [15], or the second-order coherence theory for nonstationary light [16].

From a different perspective, we recently provided a nonequilibrium thermodynamic formulation of SC generation on the basis of the wave turbulence (WT) theory [17–20]. In this framework, the spectral broadening process inherent to SC generation can be interpreted as a consequence of the natural thermalization of the optical field to the state of thermodynamic equilibrium. Although originally formulated for the description of forced-dissipative turbulent systems, the kinetic equations of the WT theory also describe the nonequilibrium evolution of random nonlinear waves in a conservative and reversible (Hamiltonian) system. In analogy with the kinetic gas theory, an isolated system of incoherent nonlinear waves exhibits, as a rule, a process of thermalization, which is characterized by an irreversible evolution of the wave system toward a thermodynamic equilibrium state, i.e., the Rayleigh-Jeans (RJ) distribution that realizes the maximum of nonequilibrium entropy [21, 22]. This irreversible behavior is expressed by a  $H$ -theorem of entropy growth [22], in analogy with the celebrated Boltzmann  $H$ -theorem relevant for gas kinetics. The kinetic wave equations then provide a detailed description of the nonequilibrium properties of this process of thermalization.

Our aim in this Brief Report is to show that this irre-

versible process of wave thermalization to the RJ spectrum can be truncated within some specific frequency interval. We consider a PCF whose dispersion curve is characterized by two ZDWs, so that the essential properties of light propagation in this fiber can be modelled by the nonlinear Schrödinger (NLS) equation including fourth-order dispersion effects [23]. In these conditions, the kinetic wave theory reveals the existence of an irreversible evolution toward a RJ equilibrium state characterized by a compactly supported spectral shape. This phenomenon of truncated thermalization can shed new light on the mechanisms underlying the formation of bounded spectra in SC generation [12, 13, 18].

Besides its natural relevance in the context of SC generation, this phenomenon is also important from a fundamental point of view. It is indeed well-known that the thermodynamic equilibrium state of a system of classical waves (i.e., RJ spectrum) is not properly defined, in the sense that it leads to diverging expressions for the power or the energy at equilibrium. This problem refers to the well-known ‘ultraviolet catastrophe’, which was originally solved by the Planck law and subsequently by a self-consistent thermodynamic formulation of quantum electromagnetic radiation. On the other hand, when one deals with an ensemble of classical optical waves, such a divergence is regularized by a frequency cut-off, which is often introduced in a rather artificial way [17, 18, 24], although it can be justified in some particular cases [25]. In this work we show how a genuine frequency cut-off arises naturally in a system of classical waves described by the generalized NLS equation accounting for higher-order dispersion effects.

*Model.*— We consider the dimensionless NLS equation accounting for third- and fourth-orders dispersion effects

$$i\partial_z\psi = -\sigma\partial_t^2\psi + i\alpha\partial_t^3\psi + \beta\partial_t^4\psi + |\psi|^2\psi. \quad (1)$$

We normalized the problem with respect to the nonlinear length  $L_0 = 1/(\gamma P)$  and the ‘healing time’  $\tau_0 = (|\beta_2|L_0/2)^{1/2}$ , where  $\gamma$  is the nonlinear coefficient,  $P$  the average power of the wave,  $\beta_2$  the second-order dispersion coefficient with  $\sigma = \text{sign}(\beta_2)$ . In these units, the normalized dispersion parameters read  $\alpha = \beta_3/(6\tau_0^3)$ , and  $\beta = \beta_4/(24\tau_0^4)$ ,  $\beta_3$  and  $\beta_4$  being the third- and fourth-order dispersion coefficients. The NLS Eq.(1) conserves three important quantities, the normalized power  $N = \int |\psi(t)|^2 dt$ , the momentum  $M = \int \omega |\tilde{\psi}(\omega)|^2 d\omega$  and the total ‘energy’ (Hamiltonian)

$H = E + U$ , which has a linear (dispersive) kinetic contribution  $E(z) = \int k(\omega) |\tilde{\psi}(\omega)|^2 d\omega$  and a nonlinear contribution  $U(z) = \frac{1}{2} \int |\psi(t)|^4 dt$ , where  $k(\omega) = \sigma\omega^2 + \alpha\omega^3 + \beta\omega^4$  is the dispersion relation  $[\tilde{\psi}(z, \omega) = \frac{1}{\sqrt{2\pi}} \int \psi(z, t) \exp(-i\omega t) dt]$ .

*Simulations.*— We recall that for  $\alpha = \beta = 0$ , Eq.(1) recovers the integrable NLS equation, which does not exhibit wave thermalization [3]. The introduction of third-order dispersion ( $\alpha \neq 0$ ) leads to a process of anomalous thermalization toward an equilibrium state of a different nature than the RJ distribution [2]. The influence of higher-order dispersion on wave thermalization was considered in the context of SC generation through the analysis of the generalized NLS equation [17, 18, 20]. Here, we revisit these previous works *by truncating the dispersion relation of the generalized NLS equation up to the fourth-order polynomial*.

The initial condition considered in the simulations is a *coherent* cw-pump wave, whose wavelength lies between the ZDWs in the anomalous dispersion regime. We report in Fig. 1 a typical evolution of the spectrum during the propagation which has been obtained by solving the NLS Eq.(1). In this example, we considered a relatively high pump power (200W), which is in the range of the powers considered in the experiments reported in Refs.[18, 20]. In this highly nonlinear regime the optical field exhibits rapid and random temporal fluctuations, which prevent the formation of robust and persistent coherent soliton structures. The optical field then exhibits an incoherent turbulent dynamics, in which coherent soliton and dispersive waves do not play a significant role, as previously discussed in high-power cw-SC generation Refs.[17, 18, 20, 26].

In this incoherent regime, the central part of the SC spectrum relaxes toward the RJ distribution, as predicted by the kinetic wave theory (see Fig. 1a). The RJ spectrum is characterized by a double peaked structure, which results from the presence of two ZDWs in the dispersion curve of the PCF (see Fig. 1c) [17, 18]. However, a careful analysis reveals the remarkable aspect that this thermalization process is not achieved in a complete fashion: The *tails* of the SC spectrum are characterized by abrupt spectral edges, which are preserved for long propagation lengths and thus do not relax toward the expected RJ spectral tails. Our aim in this paper is to grasp the physical origin of such abrupt spectral edges in the generated SC spectrum.

*Kinetic approach: RJ spectrum.*— The kinetic theory relies on a natural asymptotic closure of the hierarchy of moments equations which is induced by the dispersive properties of the waves [22]. Then assuming that the random nonlinear wave evolves in the weakly nonlinear regime,  $|U/E| \ll 1$ , the wave statistics turns out to be Gaussian, which leads to an irreversible kinetic equation describing the evolution of the averaged spectrum of the wave,  $n(z, \omega)\delta(\Omega) = \langle \tilde{\psi}(\omega + \Omega/2) \tilde{\psi}^*(\omega - \Omega/2) \rangle$  [17, 21, 22]

$$\partial_z n(z, \omega) = \text{Coll}[n], \quad (2)$$

where the collision term  $\text{Coll}[n] = \frac{1}{\pi} \int d\omega_{1,2,3} W \mathcal{N}_{\omega_1\omega_2\omega_3}(\mathbf{n})$  provides a kinetic description of the Kerr

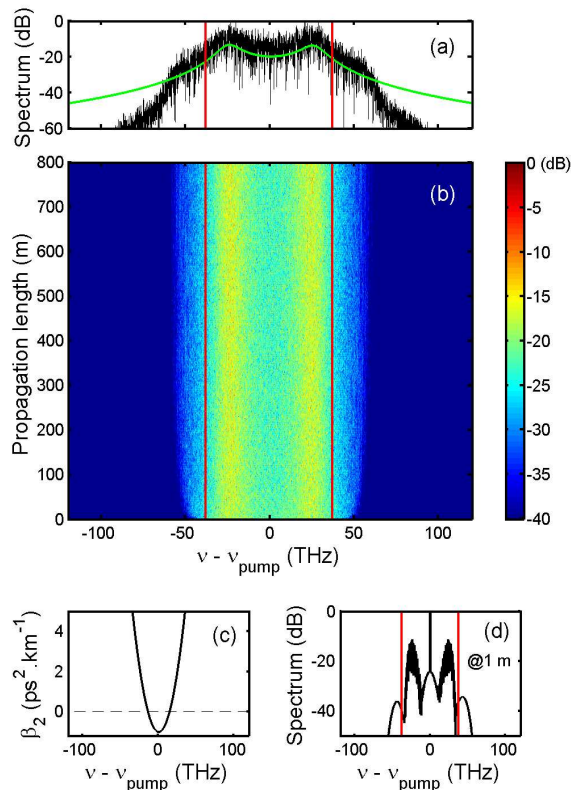


FIG. 1: (a) Numerical simulation of the NLS Eq.(1) showing the evolution of the spectrum  $|\tilde{\psi}|^2(\omega, z)$  during the propagation (in dimensional units). (b) Comparison of  $|\tilde{\psi}|^2(\omega, z)$  with the corresponding RJ spectrum [Eq.(3)]. (c) Dispersion curve of the PCF. (d) MI spectrum after 1m of propagation through the PCF. The vertical red lines denote the frequency bounds,  $\omega_{\pm}$ , given by Eq.(7). Corresponding normalized parameters:  $\sigma = -1$ ,  $\alpha = -0.0453$ ,  $\beta = 0.4186$ .

effect in Eq.(1), with  $\mathcal{N}_{\omega_1\omega_2\omega_3}(\mathbf{n}) = n(\omega) n(\omega_1) n(\omega_2) n(\omega_3) [n^{-1}(\omega) + n^{-1}(\omega_1) - n^{-1}(\omega_2) - n^{-1}(\omega_3)]$ . The phase-matching conditions underlying the four-wave mixing are expressed by the Dirac  $\delta$ -functions in  $W = \delta(\omega + \omega_1 - \omega_2 - \omega_3) \delta[k(\omega) + k(\omega_1) - k(\omega_2) - k(\omega_3)]$ . The kinetic Eq.(2) conserves the densities of power,  $N_0/T = \int n(z, \omega) d\omega$ , of ‘energy’  $E_0/T = \int k(\omega) n(z, \omega) d\omega$ , and of ‘momentum’  $M_0/T = \int \omega n(z, \omega) d\omega$  of the wave, where  $T_0$  denotes the numerical time window [17]. The irreversible character of Eq.(2) is expressed by a  $H$ -theorem of entropy growth,  $dS/dz \geq 0$ , where the nonequilibrium entropy reads  $\mathcal{S}(z) = \int \log[n(z, \omega)] d\omega$ . The RJ equilibrium spectrum  $n^{RJ}(\omega)$  realizing the maximum of  $\mathcal{S}[n]$ , subject to the constraints of conservation of  $E, M$  and  $N$ , is obtained by introducing the corresponding Lagrange’s multipliers,  $1/T, \lambda/T$  and  $-\mu/T$

$$n^{RJ}(\omega) = \frac{T}{k(\omega) + \lambda\omega - \mu}, \quad (3)$$

where  $T$  denotes the temperature and  $\mu$  the chemical potential by analogy with thermodynamics [22].

*Kinetic approach: Refined analysis.*— As discussed above through Fig. 1, this process of thermalization to the RJ spec-

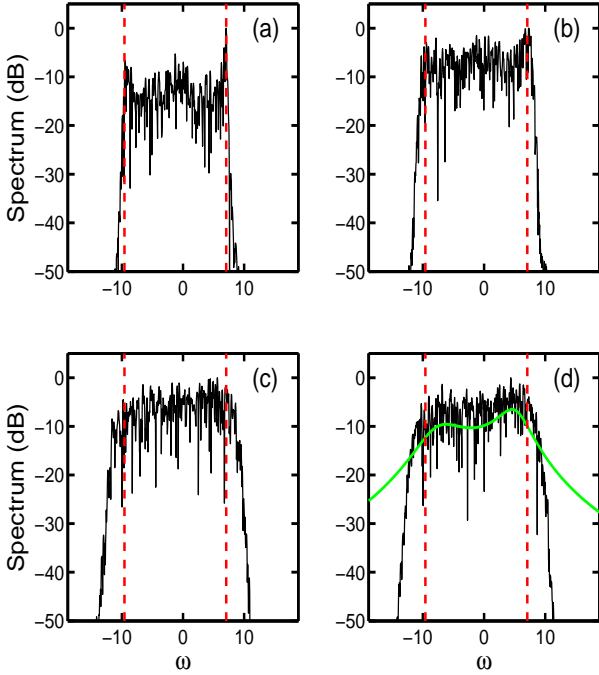


FIG. 2: Spectra  $|\tilde{\psi}|^2(\omega, z)$  in  $\text{Log}_{10}$ -scale obtained by solving the NLS Eq.(1) for  $\sigma = -1$ ,  $\alpha = 0.1$ ,  $\beta = 0.02$ : (a)  $z = 25$ , (b)  $z = 200$ , (c)  $z = 5 \times 10^5$ , (d)  $z = 10^6$ . After a long transient, the wave eventually relaxes toward a truncated RJ distribution (d).

trum (3) is not achieved in a complete way. Here we show that this effect can be described by a refined analysis of the kinetic Eq.(2). Using the property [27], we integrate the collision term of the kinetic Eq.(2) over  $\omega_1$ ,

$$\partial_z n(z, \omega) = \frac{1}{2\pi} \int \frac{\tilde{\mathcal{N}}_{\omega_2 \omega_3}(\mathbf{n})}{|\omega_2 - \omega| |\omega_3 - \omega|} \delta[\phi_\omega(\omega_2, \omega_3)] d\omega_{2,3} \quad (4)$$

where  $\tilde{\mathcal{N}}_{\omega_2 \omega_3}(\mathbf{n})$  is the functional  $\tilde{\mathcal{N}}_{\omega_1 \omega_2 \omega_3}(\mathbf{n})$  in which  $n_{\omega_1}(z)$  has been changed with  $n_{\omega_2 + \omega_3 - \omega}(z)$ , and  $\phi_\omega(\omega_2, \omega_3) = \frac{3}{2}\alpha(\omega_2 + \omega_3) + \beta[2(\omega_2^2 + \omega_3^2) + 3\omega_2\omega_3 - \omega(\omega_2 + \omega_3) + \omega^2] - 1$ . The function  $\phi_\omega(\omega_2, \omega_3)$  is a quadric in the two dimensional space  $(\omega_2, \omega_3)$ . It can be recast into its canonical form with the following change of variables: ( $\tilde{\Omega}_2 = \frac{1}{\sqrt{2}}(\omega_2 + \omega_3)$ ,  $\tilde{\Omega}_3 = \frac{1}{\sqrt{2}}(\omega_2 - \omega_3)$ ), and then ( $\tilde{\Omega}_2 = \Omega_2 + q/(7\beta)$ ,  $\tilde{\Omega}_3 = \Omega_3$ ), with  $q = 3\alpha/\sqrt{2} - \sqrt{2}\beta\omega$ . The kinetic Eq.(4) then takes the form

$$\partial_z n(z, \omega) = \int \frac{\tilde{\mathcal{N}}_{\tilde{\Omega}_2 \tilde{\Omega}_3}(\mathbf{n}) \delta[(\tilde{\Omega}_2/a_2)^2 + (\tilde{\Omega}_3/a_3)^2 - \rho]}{\pi |\tilde{\Omega}_2 + \tilde{\Omega}_3 - r_\omega| |\tilde{\Omega}_2 - \tilde{\Omega}_3 - r_\omega|} d\tilde{\Omega}_{2,3} \quad (5)$$

where  $a_2 = \sqrt{2/(7\beta)}$ ,  $a_3 = \sqrt{2/\beta}$  and  $r_\omega = 6\sqrt{2}\omega/7 + 3\sqrt{2}\alpha/(14\beta)$ . It becomes apparent that the condition

$$\rho = 1 - \frac{3}{28}(8\beta\omega^2 + 4\alpha\omega - \frac{3\alpha^2}{\beta}) \geq 0 \quad (6)$$

must be satisfied in Eq.(5). This reveals that the resonant four-wave interaction underlying the Kerr effect can only take place within a specific frequency interval defined by the bounds,  $\omega \in [\omega_-, \omega_+]$ , with

$$\omega_\pm = -\frac{\alpha}{4\beta} \pm \frac{\sqrt{21}}{12\beta} \sqrt{3\alpha^2 + 8\beta}. \quad (7)$$

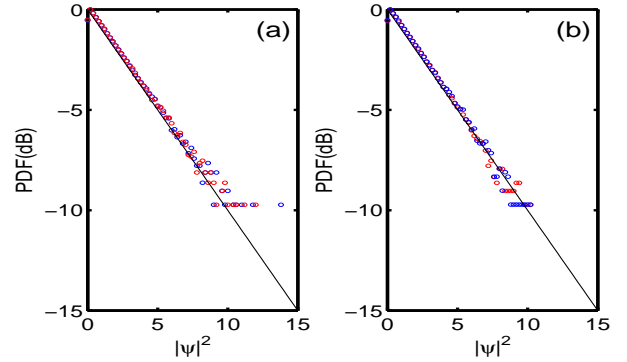


FIG. 3: (Color online) PFD of the wave intensity,  $I = |\psi|^2$ , corresponding to the simulation of Fig. 2 at  $z = 25$  (blue),  $z = 200$  (red) (a);  $z = 5 \times 10^5$  (blue),  $z = 10^6$  (blue) (b): The random wave eventually enters the kinetic regime of Gaussian statistics.

Finally remark that, by introducing the following parametrization of the ellipse, ( $\tilde{\Omega}_2 = \tilde{a}_2 \cos(\theta)$ ,  $\tilde{\Omega}_3 = \tilde{a}_3 \sin(\theta)$ ), with  $\tilde{a}_{2,3} = a_{2,3}\sqrt{\rho}$ , and making use again of the property [27], the kinetic Eq.(5) can be recast in the following compact form

$$\partial_z n(z, \omega) = \frac{\tilde{a}_2 \tilde{a}_3}{2\pi |\rho|} \int_0^{2\pi} \frac{\tilde{\mathcal{N}}_{\cos(\theta) \sin(\theta)}(\mathbf{n})}{\mathcal{F}_\omega(\theta)} d\theta, \quad (8)$$

where  $\mathcal{F}_\omega(\theta) = |\tilde{a}_2 \cos(\theta) + \tilde{a}_3 \sin(\theta) - r_\omega| \times |\tilde{a}_2 \cos(\theta) - \tilde{a}_3 \sin(\theta) - r_\omega|$ .

*Discussion.* – There is an appreciable discrepancy between the simulation of the NLS Eq.(1) reported in Fig. 1 and the frequency interval,  $\omega_\pm$ , predicted by the kinetic theory in (7). Actually, the pump power considered in Fig. 1 is quite elevated, so that the MI side-bands are located far away from the carrier pump frequency. As a result, the cascade of MI side-bands generated in the early stage of propagation go beyond the frequency interval predicted by the theory, as clearly illustrated in Fig. 1d. Since the MI process is inherently a coherent nonlinear phase-matching effect, it is not described by the kinetic Eq.(2), whose validity is restricted to the weakly nonlinear regime ( $|U/E| \ll 1$ ). This explains why the numerical simulations reported in previous works [17, 18] did not evidence a signature of this phenomenon of truncated thermalization. In order to analyze our theoretical predictions in more detail, we decreased the injected pump power so as to maintain the (cascaded) MI side-bands within the frequency interval (7).

We have performed intensive numerical simulations of the NLS Eq.(1) in this regime of reduced pump power. This study reveals that the nonlinear dynamics slows down in a dramatic way, so that the expected process of thermalization requires in fact huge nonlinear propagation lengths and huge CPU time computations. This results from the fact that the parameters  $\alpha$  and  $\beta$  decrease as the pump power decreases, so that Eq.(1) approaches the integrable limit of the NLS equation, which does not exhibit any thermalization effect [3]. We report in Fig. 2 the wave spectra at different propagation lengths obtained by solving the NLS Eq.(1) with

$\alpha = 0.1$  and  $\beta = 0.02$ . In the early stage of propagation,  $z \sim 200$ , the spectrum remains confined within the frequency interval  $[\omega_-, \omega_+]$  predicted by the theory [Eq.(7)], although the spectrum exhibits a completely different spectral profile than the expected RJ distribution. As a matter of fact, the process of thermalization requires enormous propagation lengths, as illustrated in Fig. 2d, which shows that the wave spectrum eventually relaxes toward a truncated RJ distribution. Here, the Lagrangian multipliers  $(\mu, \lambda, T)$  have been calculated from the conserved quantities  $(N, M, E)$ , without using adjustable parameters [28].

Note however in Fig. 2d that, despite the good agreement, the whole spectrum spans a frequency band which exceeds the frequency interval  $[\omega_-, \omega_+]$  predicted by the kinetic theory in Eq.(7). Indeed, in the first stage of evolution (see Fig. 2a-c for  $200 < z < 5 \times 10^5$ ), the SC spectrum exhibits a slow process of spectral broadening, so that the corresponding SC edges go beyond the frequency bound  $[\omega_-, \omega_+]$ . Such a discrepancy with the theory can be ascribed to the fact that the statistics of the wave is not strictly Gaussian. Indeed, we report in Fig. 3 the PDF of the wave intensity calculated at different propagation lengths. A deviation from Gaussian statistics is clearly visible for  $z < 200$ , which can merely explain the slow process of spectral broadening beyond the frequency interval (7) predicted by the theory. This conclu-

sion has been corroborated by the analysis of the *kurtosis of the intensity distribution*,  $K = \langle I^2 \rangle / (2 \langle I \rangle^2) - 1$  (data not shown). The value of  $K$ , as well as the variance of its fluctuations, are shown to slowly decay during the propagation to zero. Then as the system evolves, it eventually reaches a kinetic regime of Gaussian statistics, which is subsequently preserved in the further evolution. It is interesting to underline that, once the state of Gaussian statistics is reached, *the incoherent wave does not exhibit any significant spectral broadening (for  $z > 5 \times 10^5$ ), while its spectral profile slowly relaxes toward the truncated RJ distribution*, as described by the kinetic theory.

Finally note that we have performed the same numerical study for  $\alpha = 0$  (data not shown), for which the frequency bounds (7) reduce to  $\omega_{\pm} = \pm \sqrt{7/(6\beta)}$ . This study confirms the process of relaxation toward a spectrally truncated RJ distribution for the incoherent wave.

*Conclusion.*— We have reported a phenomenon of ‘truncated thermalization’ which is characterized by the formation of a RJ distribution with a compactly supported spectral shape. From a broader perspective, this work is related to the wide question underlying the physics of dynamical thermalization of nonlinear systems, in line with the Fermi-Pasta-Ulam problem [29].

- 
- [1] S. Lagrange *et al.*, Europhys. Lett. **79**, 64001 (2007); A. Picozzi *et al.*, Phys. Rev. Lett. **101**, 093901 (2008); Phys. Rev. E **72**, 046606 (2005); J. Laurie *et al.*, Phys. Rep. **514**, 121 (2012).
- [2] P. Suret *et al.*, Phys. Rev. Lett. **104**, 054101 (2010); C. Michel *et al.*, Opt. Lett. **35**, 2367 (2010).
- [3] V.E. Zakharov, Stud. Appl. Math. **122**, 219 (2009); D.B. Soh *et al.*, Opt. Express **18**, 22393 (2010); P. Suret *et al.*, Opt. Express **19**, 17852 (2011).
- [4] Y. Silberberg *et al.*, Phys. Rev. Lett. **102**, 233904 (2009).
- [5] C. Barsi, W. Wan, and J.W. Fleischer, Nature Photon. **3**, 211 (2009).
- [6] C. Conti *et al.*, Phys. Rev. Lett. **101**, 143901 (2008).
- [7] E.G. Turitsyna *et al.*, Phys. Rev. A **80**, 031804 (2009); S. Babin *et al.*, J. Opt. Soc. Am. B **24**, 1729 (2007); R. Weill, B. Fischer, and O. Gat, Phys. Rev. Lett. **104**, 173901 (2010); C. Michel *et al.*, Phys. Rev. A **84**, 033848 (2011).
- [8] A. Schwache and F. Mitschke, Phys. Rev. E **55**, 7720 (1997).
- [9] Y. Bromberg *et al.*, Nature Photon. **4**, 721 (2010).
- [10] J. M. Dudley, G. Genty, and S. Coen, Rev. Mod. Phys. **78**, 1135 (2006); J. M. Dudley and J. R. Taylor, Supercontinuum Generation in Optical Fibers (Cambridge University Press, Cambridge, 2010).
- [11] F. Biancalana *et al.*, Phys. Rev. E **68**, 046603 (2003); A. Efimov *et al.*, Phys. Rev. Lett. **95**, 213902 (2005); F. Biancalana *et al.*, Phys. Rev. E **70**, 016615 (2004); E.N. Tsouy and C.M. de Sterke, Phys. Rev. A **76**, 043804 (2007); J.C. Travers, Opt. Express **17**, 1502 (2009).
- [12] B.A. Cumberland *et al.*, Opt. Express **16**, 5964 (2008); J.C. Travers *et al.*, Opt. Express **16**, 14435 (2008).
- [13] A. Mussot *et al.*, Opt. Express **15**, 11553 (2007); S. Martin-Lopez *et al.*, Opt. Express **16**, 6746 (2008).
- [14] D.V. Skryabin and A.V. Gorbach, Rev. Mod. Phys. **82**, 1287-1299 (2010).
- [15] M. Kolesik, E. M. Wright, and J. V. Moloney, Phys. Rev. Lett. **92**, 253901 (2004).
- [16] M. Erkintalo *et al.*, Opt. Lett. **37**, 169-171 (2012).
- [17] B. Barviau, B. Kibler and A. Picozzi, Phys. Rev. A **79**, 063840 (2009).
- [18] B. Barviau *et al.*, Opt. Express **17**, 7392 (2009).
- [19] C. Michel, B. Kibler, A. Picozzi, Phys. Rev. A **83**, 023806 (2011).
- [20] B. Kibler *et al.*, Phys. Rev. E **84**, 066605 (2011).
- [21] For a simple introduction to WT in optics, see, e.g., A. Picozzi, Opt. Express **15**, 9063 (2007); J. Garnier *et al.*, J. Opt. Soc. Am. B **29**, 2229 (2012).
- [22] V.E. Zakharov, V.S. L'vov and G. Falkovich, *Kolmogorov Spectra of Turbulence I* (Springer, Berlin, 1992); A.C. Newell, S. Nazarenko, L. Biven, Physica D **152**, 520 (2001).
- [23] G. P. Agrawal, *Nonlinear Fiber Optics* (Academic Press, 5th Ed., 2012).
- [24] C. Connaughton *et al.*, Phys. Rev. Lett. **95**, 263901 (2005); M.J. Davis *et al.*, Phys. Rev. Lett. **87**, 160402 (2001).
- [25] P. Aschieri *et al.*, Phys. Rev. A **83**, 033838 (2011).
- [26] W. J. Wadsworth *et al.*, Opt. Express **12**, 299 (2004).
- [27] We made use of the property  $\int \delta(f) \gamma(x) dx = \int_S \gamma(x) / |\nabla f| dS$ , where  $S$  is the hypersurface  $f = 0$ .
- [28] The parameters  $(\mu, \lambda, T)$  have been calculated with the frequency cut-off  $\tilde{\omega}_- = -12.5$  and  $\tilde{\omega}_+ = 9.5$ , which closely correspond to the SC frequency bounds.
- [29] *The Fermi-Pasta-Ulam Problem: A Status Report*, Ed. by G. Gallavotti, Lect. Notes in Phys. (Springer, N.Y., 2007).